Spin State Tunes Oxygen Atom Transfer towards Fe IV O Formation in Fe II Complexes

Carmen E. Castillo, Ilaria Gamba, Laia Vicens, Martin Clémancey, Jean-Marc Latour, Miquel Costas, Manuel G. Basallote

Spin state tunes oxygen atom transfer towards $Fe^{IV}O$ formation in Fe^{II} complexes

Carmen E. Castillo,[a] Ilaria Gamba,[b] Laia Vicens,[b] Martin Clémancey,[c] Jean-Marc Latour,[c] Miquel Costas,*[b] and Manuel G. Basallote,*[a]

[a] Dr. C. E. Castillo, Prof. Dr. M. G. Basallote
Departamento de Ciencia de los Materiales e Ingeniería Metalúrgica y Química Inorgánica
Facultad de Ciencias, Instituto de Biomoléculas (INBIO)
Universidad de Cádiz,
Puerto Real, Cádiz 11510, Spain
E-mail: manuel.basallote@uca.es

[b] Dr. I. Gamba, L. Vicens, Prof. Dr. M. Costas
Grup de Química Bioinspirada, Supramolecular i Catàlisi (QBIS-CAT)
Institut de Química Computacional i Catàlisi (IQCC)
Departament de Química
Universitat de Girona
Campus de Montilivi, Girona E17071, Catalonia, Spain
Miquel.costas@udg.edu

[c] Dr. M. Clémancey, Prof. Dr. J.-M. Latour
CEA, CNRS, IRIG, DIESE, LCBM
Univ. Grenoble Alpes
pmb, F-38000 Grenoble, France

Supporting information for this article is given via a link at the end of the document.

Abstract: Oxo-iron(IV) complexes bearing tetradentate ligands have been extensively studied as models for the active oxidants in non heme iron dependent enzymes. These species are commonly generated by oxidation of their ferrous precursors. The mechanisms of these reactions have been seldom investigated. In this work, the kinetics of reaction of complexes $[Fe^{II}(CH_3CN)_2L](SbF_6)_2$ (**[1](SbF$_6$)$_2$** and **[2](SbF$_6$)$_2$**) and $[Fe^{II}(CF_3SO_3)_2L]$ (**[1](OTf)$_2$** and **[2](OTf)$_2$** (**1**, L = ^{Me,H}Pytacn, **2**, L = ^{nP,H}Pytacn, where $^{R,R'}$Pytacn = 1-[(6-R'-2-pyridyl)methyl]-4,7-di-R-1,4,7-triazacyclononane)) with Bu_4NIO_4 to form the corresponding $[Fe^{IV}(O)(CH_3CN)L]^{2+}$ (**3**, L = ^{Me,H}Pytacn, **4**, L = ^{nP,H}Pytacn) species has been studied in acetonitrile/acetone mixtures at low temperatures. The reactions occur in a single kinetic step with activation parameters independent of the nature of the anion and similar to those obtained for the substitution reaction using Cl^- as entering ligand, which indicates that formation of $[Fe^{IV}(O)(CH_3CN)L]^{2+}$ is kinetically controlled by substitution in the starting complex to form $[Fe^{II}(IO_4)(CH_3CN)L]^+$ intermediates that convert rapidly to the oxo complexes **3** and **4**. The kinetics of the reaction is strongly dependent on the spin state of the starting complex. A detailed analysis of the magnetic susceptibility and kinetic data for the triflate complexes reveals that the experimental values of the activation parameters for both complexes are the result of a partial compensation of the contributions from the thermodynamic parameters for the spin crossover equilibrium and the activation parameters for substitution. The observation of these opposite and compensating effects by modifying the steric hindrance at the ligand illustrates so far unconsidered factors governing the mechanism of oxygen atom transfer leading to high valent iron-oxo species.

Introduction

Oxo-iron(IV) complexes constitute the oxidizing agent in a number of non heme iron dependent enzymes that carry out a diverse array of oxidation reactions with implications in important biological and technological processes such as metabolic paths, bioremediation, DNA repair or sensing, to name a few.[1] This has prompted an interest to prepare and study the structural, spectroscopic and chemical reactivity of synthetic oxoiron(IV) bearing a wide diversity of ligand platforms among which, N-based tetra and pentadentate ligands have become largely dominant.[2] In general, oxoiron(IV) complexes are most conveniently prepared by oxidation of the corresponding ferrous precursors, and several oxidation methods have been explored including chemical oxidation with single and two electron chemical oxidants, dioxygen, electrochemical oxidation and also photochemical methods.[2] The mechanisms by which these reactions proceed may be quite diverse and dependent on the oxidant and specific complex studied but they have been only rarely investigated. Sequential single electron oxidation from Fe(II) to Fe(IV) has been documented,[3] even when two e- oxidants are employed. In some other cases, reactions have been understood to proceed via a two e- oxygen atom transfer (OAT),[4] a reaction that is mechanistically interesting because it avoids the single electron reactions commonly occurring in first row transition metal complexes and the intermediate formation of ferric compounds, often regarded as thermodynamic sinks.

However, to the best of our knowledge, the latter OAT reaction mechanism has never been clarified.

On the other hand, the role of spin state in the oxidation reactivity of oxoiron(IV) species in heme and nonheme enzymes and model systems has been extensively discussed.[5] However, to the best of our knowledge, the impact of spin state in their mechanisms of formation has not been explored.

In this work we have explored the mechanism of formation of oxoiron(IV) species in complexes bearing a tetradentate N-based ligand, by reaction of the corresponding ferrous complexes with IO_4^-. This oxidant was initially employed in the frame of catalytic water oxidation reactions,[6] where it proved to be particularly convenient for maximizing turnover numbers because it does not impose strongly acidic conditions, limiting catalyst degradation. In the specific case of iron catalyzed water oxidation reactions, oxoiron(IV) complexes were spectroscopically detected. [6-7] On the other hand, IO_4^- can be considered as a particularly more convenient "oxo transfer" agent with regard to other oxidants commonly employed to prepare oxoiron(IV) complexes such as iodosyl arenes, peroxides or NaOCl because it is commercially available in the form of pure, room temperature stable salts, soluble in organic and water media (Bu_4NIO_4 and $NaIO_4$, respectively). It also has a well-defined molecular structure and it rarely engages in single electron oxidation processes.[8] The sum of these factors led us to consider this oxidant as a paradigmatic "oxo transfer" agent to engage in a mechanistic study of the oxygen atom transfer reaction by kinetic methods.

In the present work the reactivity with IO_4^- of the complexes $[Fe^{II}(CF_3SO_3)_2(^{Me,H}Pytacn)]$ (^{Me,H}Pytacn: 1-(2'-pyridylmethyl)-4,7-dimethyl-1,4,7-triazacyclononane, **[1](OTf)$_2$**, $[Fe^{II}(CH_3CN)_2(^{Me,H}Pytacn)](SbF_6)_2$ **[1](SbF$_6$)$_2$** and the analogues with the N-methyl groups substituted by neopentyl groups $[Fe^{II}(CF_3SO_3)_2(^{nP,H}Pytacn)]$ (^{nP,H}Pytacn = 1-(2'-pyridylmethyl)-4,7-dineopentyl-1,4,7-triazacyclononane, **[2](OTf)$_2$** and $[Fe^{II}(CH_3CN)_2(^{nP,H}Pytacn)](SbF_6)_2$, **[2](SbF$_6$)$_2$** has been studied (Scheme 1). In all cases formation of the corresponding $[Fe^{IV}(O)(CH_3CN)L]^{2+}$ species (**3**, L = ^{Me,H}Pytacn and **4**, L = ^{nP,H}Pytacn) is observed, and kinetic studies provide useful information about their mechanism of formation that includes the effect of the steric constrains imposed by the alkyl substituents at the macrocyclic ligand, the ancillary ligand (X), and the spin state of the starting Fe^{II} complex.

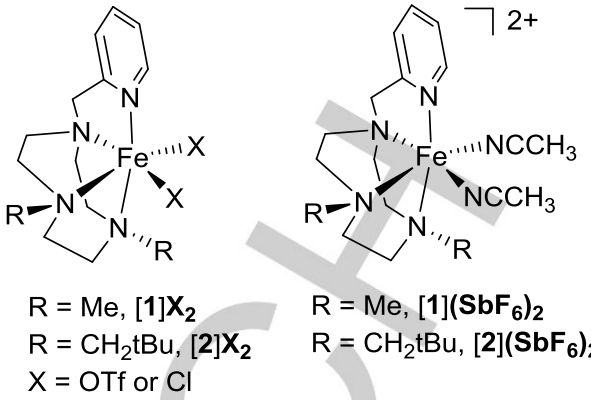

Scheme 1. Complexes studied.

Results and Discussion

Synthesis and structural characterization

Complexes $[Fe^{II}(CF_3SO_3)_2(^{Me,H}Pytacn)]$, **[1](OTf)$_2$** and $[Fe^{II}(CH_3CN)_2(^{Me,H}Pytacn)](SbF_6)_2$, **[1](SbF$_6$)$_2$** were previously described, and their solid state X-ray structure determined.[9] The ^{Me,H}Pytacn ligand platform is robust to oxidative conditions and forms highly stable iron complexes against oxidative and hydrolytic degradation. These aspects combine with a strong sigma donating ability, which results in a suitable platform for generating room stable oxo-iron(IV) complexes even in the presence of a *cis*-labile site available for external substrate binding.[3e, 10]

Complexes $[Fe^{II}(CF_3SO_3)_2(^{nP,H}Pytacn)]$, **[2](OTf)$_2$** and $[Fe^{II}(CH_3CN)_2(^{nP,H}Pytacn)](SbF_6)_2$, **[2](SbF$_6$)$_2$** were designed in order to provide a sterically shielded platform for generating high valent iron-oxo species. The molecular structure of **[2](OTf)$_2$** is shown in Figure 1. The complex bears strong similarity with the parent **[1](OTf)$_2$**,[9b] and Fe-N bond distances ~ 2.2Å are indicative of a high spin ferrous complex.[11]

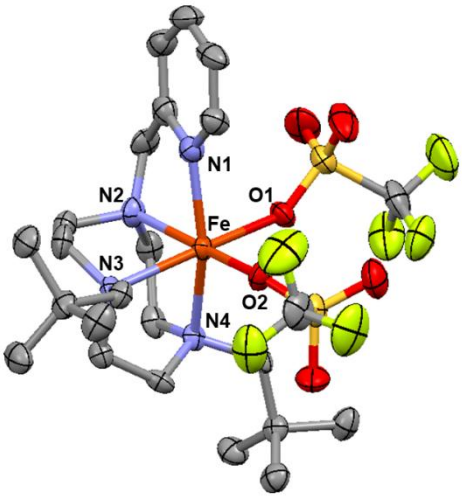

Figure 1. ORTEP diagram (50% probability level) of the X-ray structure of [2](OTf)$_2$. Selected bond distances (Å); Fe-N1, 2.154, Fe-N2, 2.188, Fe-N3, 2.273, Fe-N4, 2.248, Fe-O1, 2.157, Fe-O2, 2.047. Hydrogen atoms have been omitted for clarity.

In acetonitrile solution, **[1](OTf)$_2$** and **[2](OTf)$_2$** replace the labile triflate anions by acetonitrile ligands forming cationic bis-solvato $[Fe^{II}(CH_3CN)_2(L)]^{2+}$ L = ^{Me,H}Pytacn and ^{nP,H}Pytacn complexes.[11b, 12] In CD_3CN solution, the two complexes exhibit differences in their spin state behavior, as best shown by their molar susceptibility data determined by the Evans' method. At 298K, **[1](OTf)$_2$** and **[2](OTf)$_2$** exhibit values of χ_mT of 0.27 and 2.12 cm^3 mol^{-1} K, respectively, indicating that the former exists mainly ~~basically~~ in its low spin state, while the latter is basically high spin. In addition, temperature dependent measurements are indicative of incomplete spin crossover phenomena for the two complexes. In the case of **[1](OTf)$_2$** a diamagnetic behavior is determined below 275K, consistent with a compact spectral window from 0 to 10 ppm, displaying well-resolved ^{1}H-NMR signals. At this point, as the temperature is increased so does the χ_mT product up to 1.66 cm^3 mol^{-1} K at 340K, the highest temperature for which the experiment is possible. This behavior is indicative of an incomplete transition to the high spin state, for which a theoretical value close to 3 is expected. Instead, the spectrum of **[2](OTf)$_2$** at 298K (Figure S1) expands from 1 to 140 ppm, with relatively broad signals, indicative of a paramagnetic molecule. Its χ_mT values are consistently larger than ~~the value~~ those of **[1](OTf)$_2$**; at 298 K a value of 2.12 cm^3 mol^{-1} K ~~μ_{eff} = 4.0 MB~~ is measured, that decreases as the temperature is decreased. However, at 230K, the lowest temperature that could be accessed in CD_3CN, the measured value of 0.35 cm^3 mol^{-1} K indicates that a full transition to the low spin diamagnetic state is not accomplished. In sharp contrast, the χ_mT values exhibited by $[Fe^{II}(Cl)_2(^{nP,H}Pytacn)]$, **[2]Cl$_2$** at all temperatures are typical of a S = 2 paramagnetic molecule, although there is a noticeable decrease~~s~~ with temperature from 3.19 cm^3 mol^{-1} K at 230K down to 2.88 cm^3 mol^{-1} K at 310K, that cannot be explained by a simple Curie behavior and may be tentatively explained instead because of partial exchange of chloride by acetonitrile ligands. The weak field nature of the chloride ligands accounts for the consistent high spin nature of **[2]Cl$_2$**.

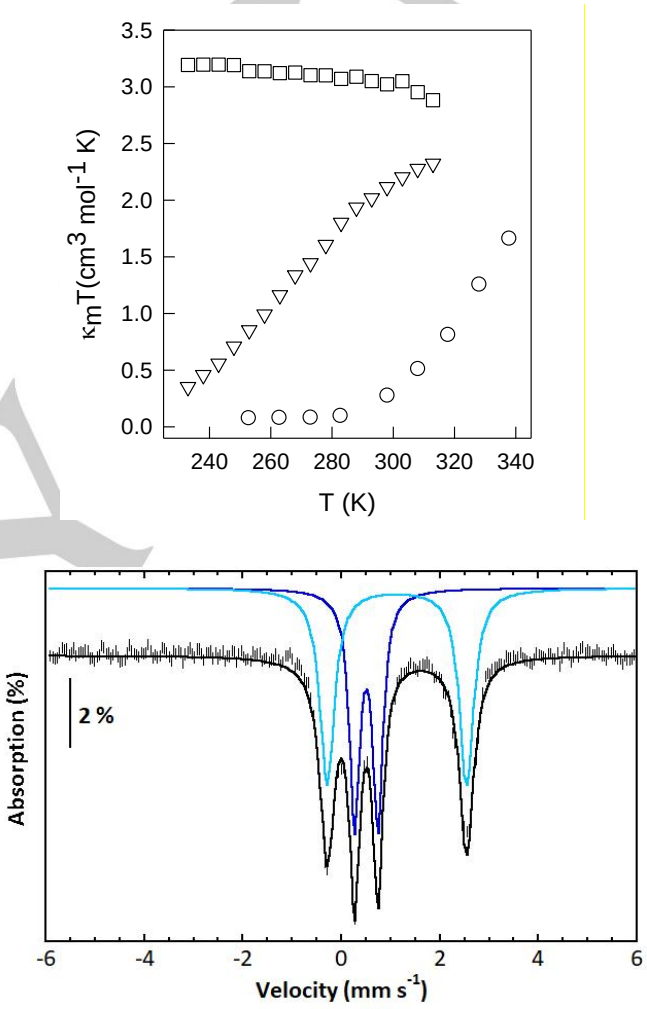

Figure 2. Top: Temperature dependence of χ_mT ~~magnetic moments measured~~ for the complexes **[1](OTf)$_2$** (circles), **[2](OTf)$_2$** (triangles) and **[2]Cl$_2$** (squares) by using the Evans method. Bottom: Mössbauer spectrum of **[2](OTf)$_2$** recorded in acetonitrile at 80 K in absence of magnetic field. (Vertical bars: experimental spectrum, solid line: calculated spectrum; see text for values of isomer shift and quadrupole splitting).

Mössbauer spectrum of a frozen sample of **[2](OTf)$_2$** in acetonitrile has been recorded at 80 K in absence of external magnetic field (Figure 2 bottom). The spectrum of **[2](OTf)$_2$** is composed of two doublets of similar intensities associated to two different Fe(II) sites. The more intense one (55 %, dark blue line) with an isomer shift δ = 0.50 mm s^{-1} and a quadrupole splitting ΔE_Q = 0.47 mm s^{-1} corresponds to a low-spin S = 0 ferrous

center. By contrast, the minor one (45 %, light blue line) with an isomer shift δ = 1.12 mm s^{-1} and a quadrupole splitting ΔE_Q = 2.83 mm s^{-1} corresponds to a high-spin S = 2 ferrous center. These data indicate that upon freezing the iron complex is trapped in two different forms. Of notice, the intensity of the high spin component at 80 K is much larger than expected from extrapolation of the magnetic moment data collected in solution, which suggests that spin crossover coexists with a different chemical process. Whereas the low spin component can be assigned to the strong field acetonitrile bound complex $[Fe^{II}(CH_3CN)_2(^{nP,H}Pytacn)](CF_3SO_3)_2$, reasonable possibilities for the high spin component are a pentacoordinated complex resulting from dissociation of one acetonitrile ligand, and a species containing coordinated triflate resulting from partial or total substitution of acetonitrile by the weak field triflate ligands.

Summarizing, the data indicates that the spin crossover observed for **[2](OTf)$_2$** in acetonitrile solution coexists with some kind of ligand exchange or dissociation. Furthermore, we also conclude that the ^{nP,H}Pytacn ligand exerts a weaker crystal field than ^{Me,H}Pytacn, despite the alkylated N atoms are better sigma donors in the former. Presumably, the steric demand of the 2,2'-dimethyl-propyl substituents prevent the tacn cycle to adopt a more compact conformation required for shortening Fe-N_{tacn} bonds.

Generation of oxoiron(IV) complexes by reaction with Bu_4NIO_4. Reaction of [**1**]**(OTf)$_2$** and [**2**]**(OTf)$_2$** (scheme 1) with one equivalent of tetrabutyl ammonium periodate (TBAP), in acetonitrile at -40 ºC, resulted in the immediate generation of $[Fe^{IV}(O)(L)(S)]^{2+}$, L = ^{Me,H}Pytacn, [**3**], and L = ^{nP,H}Pytacn [**4**] (Scheme 1). [**3**] was previously described but [**4**] is characterized for the first time in this work.[3e] The UV-Vis spectra of [**4**] features the low energy visible absorption band at λ_{max} = 760 nm, ε = 280 M^{-1}. cm^{-1} characteristic of S = 1 oxoiron(IV) complexes.[2a, 13] The formulation of [**4**] was further supported by Mössbauer spectroscopy and high-resolution cryospray mass spectroscopy (CSI-MS). Samples for Mössbauer spectroscopy were prepared by generating [**4**] in the presence of CF_3SO_3H (0.9 equiv.) because in these acidic conditions the decay of [**4**] is slower. We notice that the stability of [**3**] is also improved in the former acidic conditions.

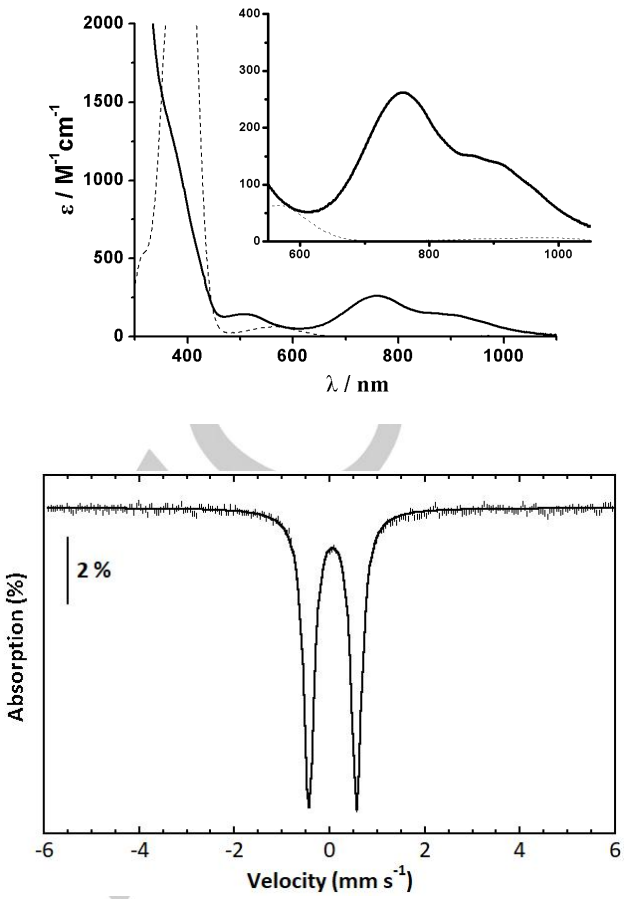

Figure 3. Figure Top: UV-Vis spectrum of **[4]** (solid line, 1 mM, acetonitrile, -40 ºC) recorded upon oxidation of **[2](OTf)$_2$** (dotted line) with 1 equivalent of NBu_4IO_4. Bottom: Mössbauer spectrum of **[4]** in acetonitrile, recorded at 80 K. (Vertical bars: experimental spectrum, solid line: calculated spectrum using the following values of isomer shift and quadrupole splitting δ = 0.06 mms^{-1} and ΔE_Q = 1.00 mms^{-1}).

CSI-MS analyses of acetonitrile solutions of **[4]** shows an intense peak at m/z = 581.2038 with an isotopic pattern fully consistent a $[[Fe^{IV}(O)(^{nP,H}Pytacn)](CF_3SO_3)]^+$ formulation (see supporting information; Figures S5-S7). The nature of S, the sixth ligand in the coordination sphere, in these complexes cannot be unambiguously established but it is likely to be an acetonitrile ligand, easily lost in the mass spectrometer, on the basis of literature precedents for reported oxoiron complexes with tetradentate ligands.[3e, 14] In the absence of a magnetic field, the Mössbauer spectrum of [**4**] (Figure 3, bottom), generated from 1 equiv. of Bu_4NIO_4 is constituted by a single doublet. Most remarkably, the spectrum shows that [**4**] is generated in a quantitative manner by using 1 equiv. of Bu_4NIO_4 and is the only iron component in the sample. This doublet is characterized by a low isomer shift δ = 0.06 mm s^{-1} and a moderate quadrupole splitting ΔE_Q = 1.00 mm s^{-1} which match the parameters generally associated to a center with an S = 1 spin state for these kinds of complexes.[2a]

Kinetic analysis of the reaction of the complexes with Bu_4NIO_4 by Stopped-flow UV-vis Spectroscopy

The reaction of ferrous complexes [**1**]$\mathbf{X_2}$ and [**2**]$\mathbf{(X)_2}$ (X = OTf and SbF_6) with $NaIO_4$ to form the corresponding oxoiron(IV) complexes **3** and **4**, were analyzed by kinetic methods using UV-Vis spectroscopy. Preliminary kinetic experiments showed that the reaction of some of the complexes with Bu_4NIO_4 to form the corresponding oxoiron(IV) species is very fast in acetonitrile solution even at the lowest temperatures achievable in this solvent. For that reason, the kinetic studies were carried out in acetonitrile/acetone (1/1) mixtures, which allow achieving lower temperatures. In all cases the spectral changes (Figure 4 shows a representative case) showed the disappearance of the band at 380-420 nm of the Fe^{II} complexes with appearance of the band typical of the $Fe^{IV}(O)$ species. Those spectral changes could be satisfactorily fitted by a model with a single kinetic step (see traces in Figure S5) that yields values of the observed rate constants (k_{obs}) that change linearly with the IO_4^- concentration (Figure 5). The rate law is thus given by equation 1; the values of the second order rate constant (k) at different temperatures are included in Table S1, and the value at -50ºC is shown in Table 1 with the corresponding activation parameters.

$$-\frac{d[complex]}{dt} = k\,[complex]\,[IO_4^-] \qquad (1)$$

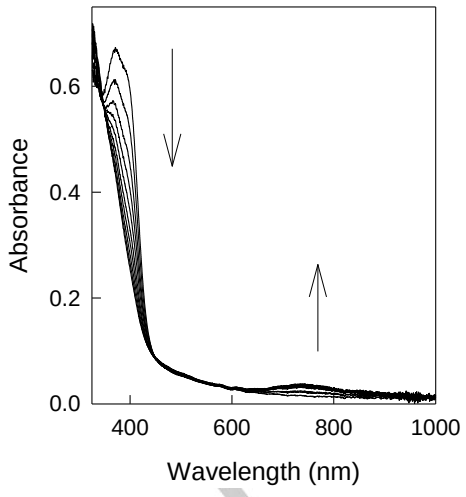

Figure 4. Spectral changes for the reaction of **[1](OTf)$_2$** (1.25×10^{-4} M) with Bu_4NIO_4 (2.5×10^{-3} M) in acetonitrile/acetone (1/1) (233 K, 0.02 M Bu_4NOTf).

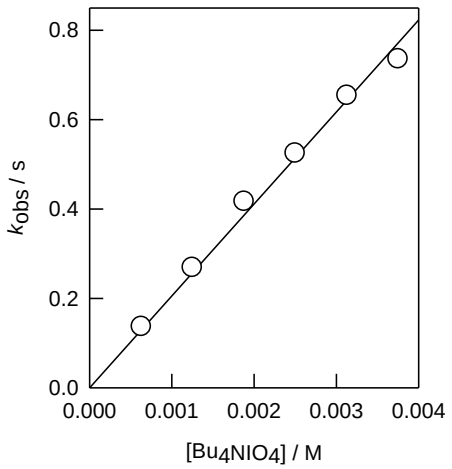

Figure 5. Kinetic data for the reaction of the **[1](OTf)$_2$** with Bu_4NIO_4 in acetonitrile/acetone (1/1) (243 K, 0.02 M Bu_4NOTf).

Table 1. Activation parameters for the reaction of the complexes with Bu_4NIO_4 or chloride in acetonitrile/acetone (1/1).

Complex	X	Reaction	k^{223}[a]	$\Delta H^{\neq}$ [b]	$\Delta S^{\neq}$ [c]
[1]X$_2$	$CF_3SO_3^-$ [d] [e]	Fe^{IV}=O formation	6.5 [f]	74±1	103±3
	SbF_6^- [g]	Fe^{IV}=O formation	18.6	75±2	117±8
	$CF_3SO_3^-$ [e]	Cl^- substitution	15.6	76±1	122±5
[2]X$_2$	$CF_3SO_3^-$ [e]	Fe^{IV}=O formation	718	59±1	76±4
	SbF_6^- [g]	Fe^{IV}=O formation	1775	59±2	84±7
	$CF_3SO_3^-$ [g]	Cl^- substitution	1796	59±2	84±7

[a] Second order rate constants (M^{-1} s^{-1}) at 223 K. Standard deviations are typically lower than 5%. [b] kJ mol^{-1}. [c] J mol^{-1} K^{-1}. Note that the uncertainties in the values are probably larger than those shown in the Table because of the relatively small temperature range used in the kinetic measurements. [d] For this reaction the activation parameters were also determined in neat acetonitrile ($\Delta H^{\neq}$ = 75±1 kJ mol^{-1} and $\Delta S^{\neq}$ = 109±2 J K^{-1} mol^{-1}), and in acetonitrile/acetone (1/1) mixture in the absence of supporting electrolyte ($\Delta H^{\neq}$ = 73±2 kJ mol^{-1} and $\Delta S^{\neq}$ = 109±4 J K^{-1} mol^{-1}). [e] in the presence of 0.02 M $(Bu_4N)(CF_3SO_3)$. [f] Value estimated from the activation parameters. [g] in the presence of 0.02 M $(Bu_4N)(PF_6)$.

In general, the rate constants for the reactions of complexes [**2**]$\mathbf{X_2}$ are about two orders of magnitude faster than those of the corresponding [**1**]$\mathbf{X_2}$, which points to a higher reactivity of the high spin forms of the complexes. With regard to the effect of X, the SbF_6^- complexes show rate constants 2-3 times larger than the corresponding triflate analogues However, these changes in the rate constants do not translate into significant changes in the activation parameters, which agree within errors for all determinations irrespective of the nature of X and supporting electrolyte. As the activation parameters derived in acetonitrile-

acetone mixtures in the absence of supporting electrolyte and in neat acetonitrile are also similar (see footnote in Table 1), it can be considered that the complexes exist in solution as bis-solvato dicationic complexes $[Fe^{II}(CH_3CN)_2(L)]^{2+}$ (L = ^{Me,H}Pytacn and ^{nP,H}Pytacn), as initially expected, although formation of minor amounts of species containing coordinated triflate cannot be completely ruled out. On the other hand, although the reactions between Bu_4NIO_4 and [**1**]**Cl₂** or [**2**]**Cl₂** show the appearance of a weak band at ca. 800 nm that suggests the formation of small amounts of $Fe^{IV}(O)$ species, they are too fast to be studied under the selected experimental conditions even using the solvent mixture. In addition, the 800 nm band disappears very rapidly even at -60ºC, which indicates the formation of unstable species that eluded spectroscopic characterization.

To obtain additional mechanistic information, the kinetics of the substitution reaction of the triflate complexes [**1**]**(OTf)₂** and [**2**]**(OTf)₂** with Pr_4NCl was studied. The spectral changes (Figure 6) show a shift of the band from 386 nm to 420 nm consistent with formation of the corresponding chloro complexes [**1**]**Cl₂** and [**2**]**Cl₂**, and they could be also fitted satisfactorily with a single kinetic step with rate constants (Table S2) and activation parameters (Table 1) similar to those derived for the reaction with IO_4^-.

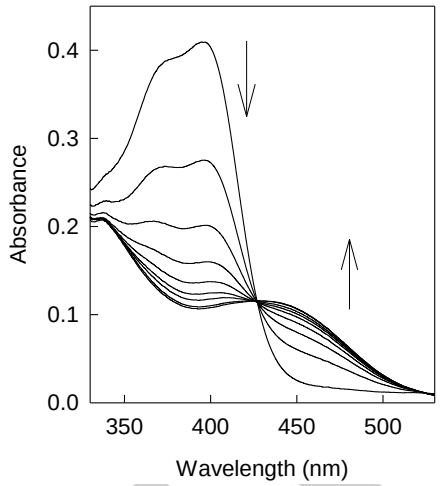

Figure 6. Spectral changes for the reaction between [**1**]**(OTf)₂** (1.5×10^{-4} M) and Pr_4NCl (3.3×10^{-3} M) in acetonitrile/acetone (1/1) (213 K, 0.02 M Bu_4NPF_6).

Mechanistic considerations

The similarity of the activation parameters for the reaction of the Fe^{II} complexes [**1**]**(X)₂** and [**2**]**(X)₂** (X = OTf and SbF_6) with Cl^- and IO_4^- strongly suggests that the formation of the corresponding $Fe^{IV}(O)^{2+}$ complexes **3** and **4** occurs through an inner sphere mechanism kinetically controlled by substitution, to form an $[Fe^{II}(IO_4)(CH_3CN)(L)]^+$ intermediate that undergoes rapidly an oxygen atom transfer to form the oxo complex. This result is in agreement with the commonly accepted proposal that periodate is an inner-sphere oxidant,[15] although comparison of the present results with literature data is hindered by the fact that most previous kinetic studies have been carried out in water, where the existence of equilibria involving formation of additional $H_{5-x}IO_6^{x-}$ octahedral species complicates the kinetics and preclude direct comparison of the data.[16]

The experimental results for the formation of $Fe^{IV}(O)^{2+}$ complexes **3** and **4** show a clear dependence of the rate constants and activation parameters with the spin state of the starting Fe^{II} complex (Figure 2). Thus, [**1**]**X₂** complexes (X= $CF_3SO_3^-$, SbF_6^-), which are low spin (LS) at all temperatures used in the kinetic studies, react more slowly than [**2**]**X₂**, which exist as an equilibrium mixture between the LS and HS (high spin) forms, and the Cl^- complexes, which are HS at all temperatures, react too fast for its kinetics to be measured. The rate constants for the reactions of [**1**]**X₂** are about two orders of magnitude lower than those of [**2**]**X₂**, which is associated mainly to a difference of c.a. 16 kJ mol^{-1} in the activation enthalpy. As the reaction is kinetically controlled by substitution and occurs in all cases in a single kinetic step independently of the existence or not of a mixture of the HS and LS forms, the present results clearly favor a mechanism in which there is an initial rapid pre-equilibrium involving spin crossover of the starting Fe^{II} complex followed by rate-limiting reaction of the more labile HS species to form an undetected $[LFe^{II}(IO_4)(CH_3CN)]^+$ intermediate that converts rapidly to $[LFe^{IV}(O)(CH_3CN)]^{2+}$ (equations 2-4). The rate law for this mechanism (equation 5) indicates that the experimental second order rate constant $k = (k_2 K_{sco})/(1 + K_{sco})$ and so the activation parameters include contributions from both the equilibrium constant K_{sco} and the rate constant k_2. In any case, the large positive activation entropies suggest a dissociative nature for the overall process represented by k.

$$[LFe^{II}(NCCH_3)_2]^{2+}{}_{LS} \rightleftarrows [LFe^{II}(NCCH_3)_2]^{2+}{}_{HS} \quad ; K_{sco} \qquad (2)$$

$$[LFe^{II}(NCCH_3)_2]^{2+}{}_{HS} + IO_4^- \xrightarrow{k_2} [LFe^{II}(IO_4)(NCCH_3)]^+ + CH_3CN \quad ; \qquad (3)$$

$$[LFe^{II}(IO_4)(NCCH_3)]^+ \rightarrow [LFe^{IV}(O)(NCCH_3)]^{2+} \quad ; \textit{fast} \qquad (4)$$

$$k_{obs} = \frac{k_2 K_{sco}}{1 + K_{sco}}[IO_4^-] \qquad (5)$$

To obtain additional information to separate the contributions from K_{sco} and k_2, the χ_mT data in Figure 2 were used to derive the values of the thermodynamic parameters for the spin crossover equilibrium. The details are given in the Supporting Information, and the thermodynamic parameters are included in Table 2. In addition, the values of k_2 at different temperatures,

and the corresponding activation parameters (Table 2), were obtained from the experimental second order rate constants by using equation 4 and the K_{sco} values derived from the magnetic susceptibility data.

Table 2. Thermodynamic parameters for the spin crossover equilibrium and activation parameters for the rate-limiting k_2 step.

	K_{sco} step		k_2 step	
Complex	ΔH_{sco} [a]	ΔS_{sco} [b]	$\Delta H_2^{\neq}$ [a]	$\Delta S_2^{\neq}$ [b]
[1](OTf)$_2$	62±4	187±13	11.5±0.7	-84±3
[2](OTf)$_2$	30±2	110±7	31±1	-25±5
Difference [c]	32±4	77±15	-20±1	-59±6

[a] kJ mol^{-1}. [b] J mol^{-1} K^{-1}. [c] Values for **[1](OTf)$_2$** minus values for **[2](OTf)$_2$**.

The values in Table 2 indicate that the spin crossover equilibrium for both complexes is characterized by positive entropy changes, as usually observed for other spin crossover complexes. However, the values of ΔH_{sco} and ΔS_{sco} are larger than those determined for iron complexes with similar coordination environment undergoing solution-phase spin change, [17] and deserve consideration. Although a detailed analysis of the spin crossover in these complexes is out of the scope of the present work, one possible explanation is that the spin transition coexists with other temperature dependent process, which would make the values in Table 2 to include contributions not only from the spin transition but also from the other process. In this sense, several examples have been reported of changes in the thermodynamic parameters for spin transitions in Fe^{II} complexes associated to different types of processes.[18] Of particular relevance to the present complexes is the related [Fe^{II}(men)(CH$_3$CN)$_2$](ClO$_4$)$_2$ (men = *N,N'*-dimethyl-*N,N'*-bis(2-pyridylmethyl)-1,2-diaminoethane, ΔH_{sco} = 39 kJ mol^{-1} and ΔS_{sco} = 134 J mol^{-1} K^{-1}) for which the large entropic change was explained by a spin-coupled dissociation of an acetonitrile ligand.[18a] Consistent with this interpretation is the MB spectrum of **[2](OTf)$_2$** recorded at 80K, which display two different spin components in a roughly 1:1 ratio. Magnetic susceptibility experiments conducted in solution state show that upon slow cooling, **[2](OTf)$_2$** transforms into a low spin complex below 200K, strongly suggesting that spin crossover in these complexes coexists with acetonitrile dissociation or ligand exchange between triflate and acetonitrile ligands, which is further supported by the observation of both kind of processes for the closely related [Fe^{II}(Me$_3$tacn)(CH$_3$CN)$_3$](CF$_3$SO$_3$)$_2$ complex in acetonitrile solution.[19]

On the other hand, the activation parameters for the k_2 step indicate a more ordered transition state for **[1](OTf)$_2$**, which indicates that the rate-limiting substitution in the HS form of this complex is more associative than for **[2](OTf)$_2$**. Actually, the large negative $\Delta S_2^{\neq}$ values in Table 2, especially for **[1](OTf)$_2$**, clearly favor an associative mechanism for the k_2 step, in which the entering ligand attacks to a pentacoordinated complex resulting from the ligand dissociation that coexists with the spin crossover equilibrium. Thus, the reaction mechanism is better formulated as indicated in Figure 7, in which the spin crossover equilibrium includes dissociation of one acetonitrile ligand, which explains the large values of ΔS_{sco}, and the k_2 step corresponds to associative attack of IO_4^- to the resulting pentacoordinated species, in agreement with the negative $\Delta S_2^{\neq}$ values. The derivation of positive activation entropies from the experimental data (Table 1) is then a consequence of the larger absolute values of ΔS_{sco} with respect to those of $\Delta S_2^{\neq}$. In addition, the $\Delta\Delta S_{sco}$ for both complexes (77 J K^{-1} mol^{-1}) is almost cancelled by $\Delta\Delta S_2^{\neq}$ (- 59 J K^{-1} mol^{-1}), and so the changes in the entropies terms do not contribute in a significant extend to the difference in k_{obs} observed for both complexes. In contrast, the differences between the spin crossover and substitution enthalpy terms ~~is~~ are larger and constitute~~s~~ the major reason for the different experimental rates of formation (k_{obs}) of the [Fe^{IV}(O)]$^{2+}$ species for both complexes.

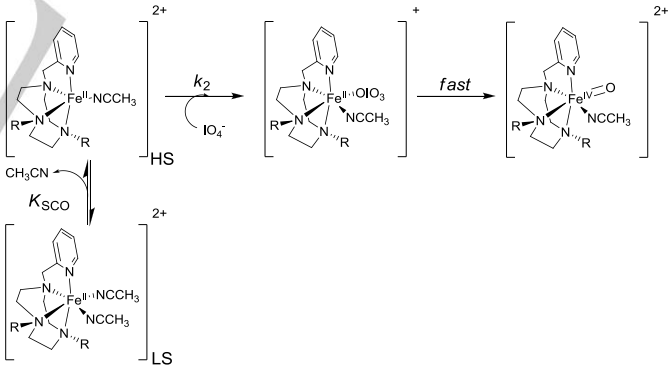

Figure 7. Mechanism proposed for the formation of the oxo-iron(IV) complexes.

In perspective, the present results illustrate the striking effect caused by replacement of methyl by neopentyl groups in the ligand. A priori one may expect that the neopentyl substituents will exert a larger inductive effect than the methyl groups, which will make the tacn N(Me)-groups a better sigma donors, in turn translating into a stronger ligand field. However, our analyses of the spin state behavior of the complexes indicate instead that the methyl substituted ^{Me,H}Pytacn ligand exerts a stronger ligand

field than ^{nP,H}Pytacn. Presumably, strain in the macrocycle caused by the alkyl substituents account for this behavior; the smaller steric effects in the methyl-containing ^{Me,H}Pytacn ligand allow for shorter metal-ligand bonds in the LS form, which causes a stronger ligand field that stabilizes LS and hinders crossover. In contrast, we propose that the steric demand of the isobutyl groups in ^{nP,H}Pytacn introduces strain in the N donors which disfavor the compression of the tacn macrocycle required to accommodate the short Fe-N distances of the low spin state.

Furthermore, the analysis of the activation parameters associated with k_2 suggests that the steric demand hinders approximation of the IO_4^- ligand and leads to a less associative character of the substitution step, as shown by the significantly less native value of the activation entropy. This imposes an increased enthalpic penalty in the activation barrier corresponding to k_2 for [**2**]**(OTf)$_2$**. However, this effect is overruled by the energetics associated with the spin crossover, which overall dominate the oxygen atom transfer reaction. Overall, these findings indicate that a simple explanation of the steric effects caused by the substituents at the ligand is not possible, as the experimental activation parameters for the formation of the oxo-iron(IV) species are the result of two opposite and partly compensating effects. In this situation, the energetics of the spin-crossover end up dominating the overall oxygen atom transfer reaction.

Conclusion

The results described in this work illustrate an interplay of subtle ligand controlled factors governs the reactivity of ferrous centers in their oxidation via an oxygen atom transfer reaction to form high-valent non-heme iron(IV)-oxo species. Comparison between **1** and **2** reveals that their spin state is a major dictating element in their rate of reaction with IO_4^- to form the corresponding oxoiron(IV) complexes **3** and **4**, respectively. This effect can be satisfactorily explained on the basis of simple ligand substitution parameters, while putative effects of the ligand in the red-ox properties of the iron center don't appear to be significant. Of interest, the differences in crystal field exerted by the tacn ligand in **1** and **2** can be explained by the strain imposed by the bulkier neopentyl arms of the tacn ligand, which disfavors the compression of the N_4Fe unit that accompanies the comparatively shorter Fe-N distances associated with the low spin state and favor the formation of labile high spin iron centers. Nevertheless, the changes in the activation parameters between different complexes can be smaller than expected from simple considerations because of partial compensation between the contributions of the spin crossover and the substitution processes to the experimentally observed activation parameters. In perspective, the current work describes a novel example where spin state plays a determining role in the reactivity of iron centers.[20] Furthermore, we suggest that the significant population of the high spin state caused by the ligand strain can be understood as an entatic state of the complex, which translates into an enhanced reactivity.[21]

Experimental Section

Materials and general.

Acetonitrile (CH_3CN, VWR, Anhydrous), tetrabutyl ammonium periodate (Bu_4NIO_4, Aldrich), tetrapropyl ammonium chloride (Pr_4NCl, Aldrich). All reagents and solvents were used as received. Ferrous complexes [**1**]**X$_2$** were synthesized according to literature precedents.[9] Magnetic measurements in acetonitrile solution were performed by the Evans' method, following previously described procedures.[11b]

Preparation and characterization of [2]X$_2$

[2](OTf)$_2$ was synthetized by mixing the ligand ^{nP,H}Pytacn, and $Fe(CF_3SO_3)_2(CH_3CN)_2$ in THF under an inert atmosphere. In an anaerobic box filled with N_2, typically 50-60 mg of the ^{nP,H}Pytacn ligand were weighed in a glass vial and dissolved in 2.0 mL of THF. Then, the desired amount of $Fe(CF_3SO_3)_2(CH_3CN)_2$ (1 equiv. respect to the ligand) was added, as solid portions, to the stirred solution. The final mixture was stirred overnight at room temperature and upon diethyl ether addition (5-6 mL), the desired bis-triflate compound **[2](OTf)$_2$** was obtained as solid precipitate. The precipitate was filtered off the mother solution, washed with diethyl ether, dissolved in the minimum amount of dichloromethane and recrystallized by slow diethyl ether diffusion, providing the corresponding complex as a crystalline material in 50-60 % yields. Elemental analysis calculated for $C_{24}H_{40}F_6FeN_4O_6S_2$; C: 40.34, H: 5.64, N: 7.84. Found; C: 40.29, H: 5.65, N: 7.89. HRMS calculated for [M+L+OTf]+ ($C_{23}H_{40}F_3FeN_4O_3S$): 565,21; Found: 565,21.

Preparation of the [**2**]**Cl$_2$** was achieved following a similar procedure: ^{nP,H}Pytacn ligand and $FeCl_2$ were mixed in CH_3CN at room temperature under a N_2 atmosphere. The final mixture was stirred overnight at room temperature and upon diethyl ether addition (5-6 mL), precipitation of the desired compound was achieved. Elemental analysis calculated for $C_{22}H_{40}Cl_2FeN_4$; C: 54.22, H: 8.27, N: 11.50. Found; C: 54.62, H: 8.20, N: 12.15.

[**2**]**(SbF$_6$)$_2$** was synthetized by mixing the ligand ^{nP,H}Pytacn and $FeCl_2$ in THF under an inert atmosphere. In an anaerobic box filled with N_2, typically 50-60 mg of the ^{nP,H}Pytacn were weighed in a glass vial and dissolved in 2.0 mL of THF. Then, the desired amount of $FeCl_2$ (1 equiv. respect to the ligand) was added, as solid portions, to the stirred solution. The final mixture was stirred overnight at room temperature. During stirring, the yellow bis-chloride compound [**2**]**(Cl)$_2$** is obtained (which partially precipitates of the THF solution). Upon diethyl ether addition (2-3 mL) the full precipitation of the [**2**]**(Cl)$_2$** complex is provoked and the solid

compound could be filtered of the solution, dried and weighted to be quantified (generally obtained in 60-70 % yield).

At this point, [**2**]**(Cl)$_2$** obtained is dissolved in acetonitrile and the desired amount of $AgSbF_6$ (two equiv. respect to the [**2**]**(Cl)$_2$** compound) was added as solid portions and the mixture stirred overnight. This reaction should be carried out in an opaque reaction flask to avoid the photo-oxidation of Ag(I), which could occur in presence of light. During the stirring the yellow color of the solution, due to the [**2**]**(Cl)$_2$** compound disappeared, while a white precipitate (AgCl) is formed. The precipitate is filtered off the mixture and the acetonitrile solution is dried under vacuum, giving the desired [**2**]**(SbF$_6$)$_2$** compound. Elemental analysis calculated for $C_{22}H_{40}F_{12}FeN_4Sb_2$; C: 29.76, H: 4.54, N: 6.31. Found; C: 31.11, H: 4.64, N: 7.31.

Generation of Fe^{IV} complexes for spectroscopic characterization.

A 2 mL acetonitrile solution containing [**1**]**(OTf)$_2$** or [**2**]**(OTf)$_2$** precursor complexes (2 μmol, 1 mM) is cooled at -40 ºC. A 50 μmol aliquot of tetrabutyl ammonium periodate (Bu_4NIO_4, 2.05 μmol) and trific acid (CF_3SO_3H, 1.5 μmol) solution was added. The resulting Fe(IV)-oxo complexes $[Fe^{IV}(O)(CH_3CN)L]^{2+}$ (**3**, L = ^{Me,H}Pytacn, **4**, L = ^{nP,H}Pytacn) instantaneously form.

The immediate generation of **[3]** and **[4]** is characterized by a low energy visible absorption band at λ_{max} = 760 nm, ε = 280 $M^{-1}cm^{-1}$ and λ_{max} = 760 nm, ε = 280 $M^{-1}cm^{-1}$, respectively.

The oxidant solution was freshly made for each experiment and prepared as follow: 36 mg Bu_4NIO_4 were dissolved in 2.45 mL CH_3CN, then 50 μL of 1.2 M CF_3SO_3H (110 μL CF_3SO_2OH up to 1 mL CH_3CN) were added to the Bu_4NIO_4 solution. Samples of **[3]** and **[4]** were analyzed by high-resolution cryospray mass spectroscopy (CSI-HRMS), exhibiting predominant peak at m/z = 469,08 and 581,20, respectively, consistent with the presence of $[Fe^{IV}(L)(O)(OTf)]^+$ ions as main species (full spectra is collected as supporting information).

Samples, prepared at 2 mM concentration, were frozen with liquid N_2 and subjected to Mössbauer spectroscopy.

Mössbauer spectroscopy.

Mössbauer spectra were recorded at 80 K on a strong-field Mössbauer spectrometer equipped with an Oxford Instruments Spectromag 4000 cryostat. The spectrometer was operated in a constant acceleration mode in transmission geometry. The isomer shifts were referenced against that of a metallic iron foil at room temperature. Analysis of the data was performed with the program WMOSS (WMOSS4 Mössbauer Spectral Analysis Software, www.wmosss.org, 2009-2015).

*Kinetics of the reaction of **[1]X$_2$** and **[2]X$_2$** with Bu_4NIO_4.*

The kinetics of reaction of the complexes with Bu_4NIO_4 were studied by recording the spectral changes with time using an SFM4000 Bio-Logic stopped-flow instrument provided with a diode-array detector and a cryo-stopped-flow accessory immersed in a Huber CC-905 bath. A 0.25 mM solution of the complexes in acetonitrile/acetone (1/1) was prepared in a glove-box, and the kinetics of reaction with the oxidant was studied using pseudo-first order conditions of oxidant excess. All kinetic experiments were carried out in the presence of 0.02 M tetrabutylammonium salt (triflate or hexafluorophosphate) as supporting electrolyte to avoid the changes in the rate constant with the ionic strength expected for a reaction between two charged species. The same procedure was used for studying the kinetics of the substitution reactions with Pr_4NCl. A global analysis of the kinetic data was carried out using the software SPECFIT.[22] The kinetics was studied at different temperatures to obtain the activation parameters using Eyring plots.

Acknowledgements

This work was supported by the Spanish Ministry of Science, Innovation and Universities (PGC2018-101737-B-I00 to M.C. and PID2019-107006GB-C22 to M.G.B.), Generalitat de Catalunya (2017 SGR 00264 and ICREA Academia Award to M.C.), the 2014-2020 ERDF Operational Programme and the Department of Economy, Knowledge, Business and University of the Regional Government of Andalusia (FEDER-UCA18-106753 to C.E.C.).

Keywords: Kinetics • Oxidation • Oxoiron(IV) • Reaction mechanisms • Spin crossover

[1] a) E. G. Kovaleva and J. D. Lipscomb, *Nature Chem. Biol.* **2008**, *4*, 186-193; b) J. M. Bollinger Jr, W.-c. Chang, M. L. Matthews, R. J. Martinie, A. K. Boal and C. Krebs in *CHAPTER 3 Mechanisms of 2-Oxoglutarate-Dependent Oxygenases: The Hydroxylation Paradigm and Beyond*, *Vol.* The Royal Society of Chemistry, **2015**, pp. 95-122; c) P. Rabe, J. J. A. G. Kamps, C. J. Schofield and C. T. Lohans, *Nat. Prod. Rep.* **2018**, *35*, 735-756.

[2] a) A. R. McDonald and L. Que, Jr., *Coord. Chem. Rev.* **2013**, *257*, 414-428; b) M. Guo, T. Corona, K. Ray and W. Nam, *Acs Cent. Sci.* **2019**, *5*, 13-28.

[3] a) X. Shan and L. Que, Jr. *Chem. Commun.* **2008**, 2209-2211; b) A. Thibon, J. England, M. Martinho, V. G. Young, J. R. Frisch, R. Guillot, J. J. Girerd, E. Munck, L. Que, Jr. and F. Banse, *Angew. Chem. Int. Ed.* **2008**, *47*, 7064-7067; c) D. C. Lacy, R. Gupta, K. L. Stone, J. Greaves, J. W. Ziller, M. P. Hendrich and A. S. Borovik, *J. Am. Chem. Soc.* **2010**, *132*, 12188–12190; d) Y.-M. Lee, S. N. Dhuri, S. C. Sawant, J. Cho, M. Kubo, T. Ogura, S. Fukuzumi and W. Nam, *Angew. Chem. Int. Ed.* **2009**, *48*, 1803-1806; e) A. Company, I. Prat, J. R. Frisch, D. R. Mas-Ballesté, M. Güell, G. Juhász, X. Ribas, D. E. Münck, J. M. Luis, L. Que, Jr. and M. Costas, *Chem. Eur. J.***2011**, *17*, 1622-1634; f) F. Li, K. K. Meier, M. A. Cranswick, M. Chakrabarti, K. M. Van Heuvelen, E. Münck and L. Que, Jr. *J. Am. Chem. Soc.* **2011**, *133*, 7256-7259; g) H. Kotani, T. Suenobu, Y.-M. Lee, W. Nam and S. Fukuzumi, *J. Am. Chem. Soc.***2011**, *133*, 3249-3251; h) F. Li, K. M. Van Heuvelen, K. K. Meier, E. Muenck and L. Que, Jr., *J. Am. Chem. Soc.***2013**, *135*, 10198-10201; i) Y. Nishida, Y.-M. Lee, W. Nam and S. Fukuzumi, *J. Am. Chem. Soc.* **2014**, *136*, 8042-8049; j) A. Company, G. Sabenya, M. Gonzalez-Bejar, L. Gomez, M. Clemancey, G. Blondin, A. J. Jasniewski, M. Puri, W. R. Browne, J. M. Latour, L. Que, Jr., M. Costas, J. Perez-Prieto and J. Lloret-Fillol, *J. Am. Chem. Soc.* **2014**, *136*, 4624-4633; k) S. Bang, S. Park, Y.-M. Lee, S. Hong, K.-B. Cho and W. Nam, *Angew. Chem. Int. Ed.* **2014**, *53*, 7843-7847.

[4] a) J. Kaizer, E. J. Klinker, N. Y. Oh, J.-U. Rohde, W. J. Song, A. Stubna, J. Kim, E. Munck, W. Nam and L. Que, Jr., *J. Am. Chem. Soc.* **2004**, *126*, 472-473; b) J. Bautz, M. R. Bukowski, M. Kerscher, A. Stubna, P. Comba, A. Lienke, E. Münck and L. Que Jr, *Angew. Chem. Int. Ed.* **2006**, *45*, 5681-5684;

c) S. Meyer, I. Klawitter, S. Demeshko, E. Bill and F. Meyer, *Angew. Chem. Int. Ed.* **2013**, *52*, 901-905; d) M. Mitra, H. Nimir, S. Demeshko, S. S. Bhat, S. O. Malinkin, M. Haukka, J. Lloret-Fillol, G. C. Lisensky, F. Meyer, A. A. Shteinman, W. R. Browne, D. A. Hrovat, M. G. Richmond, M. Costas and E. Nordlander, *Inorg. Chem.* **2015**, *54*, 7152-7164; e) S. Schaub, A. Miska, J. Becker, S. Zahn, D. Mollenhauer, S. Sakshath, V. Schünemann and S. Schindler, *Angew. Chem. Int. Ed.* **2018**, *57*, 5355-5358; f) X. Engelmann, D. D. Malik, T. Corona, K. Warm, E. R. Farquhar, M. Swart, W. Nam and K. Ray, *Angew. Chem. Int. Ed.* **2019**, *58*, 4012-4016.

[5] a) S. Shaik, M. Filatov, D. Schröder and H. Schwarz, *Chem. Eur. J.* **1998**, *4*, 193-199; b) D. Schröder, S. Shaik and H. Schwarz, *Acc. Chem. Res.* **2000**, *33*, 139-145; c) S. Shaik, S. P. de Visser, F. Ogliaro, H. Schwarz and D. Schröder, *Curr. Op. in Chem. Biol.* **2002**, *6*, 556-567; d) C. V. Sastri, J. Lee, K. Oh, Y. J. Lee, J. Lee, T. A. Jackson, K. Ray, H. Hirao, W. Shin, J. A. Halfen, J. Kim, L. Que, Jr., S. Shaik and W. Nam, *Proc. Natl. Acad. Sci. USA* **2007**, *104*, 19181-19186; e) H. Hirao, L. Que, Jr., W. Nam and S. Shaik, *Chem. Eur. J.* **2008**, *14*, 1740-1756; f) E. Andris, J. Jasik, L. Gomez, M. Costas and J. Roithova, *Angew. Chem. Int. Ed.* **2016**, *55*, 3637-3641; g) C. Kupper, B. Mondal, J. Serrano-Plana, I. Klawitter, F. Neese, M. Costas, S. F. Ye and F. Meyer, *J. Am. Chem. Soc.* **2017**, *139*, 8939-8949.

[6] a) W. C. Ellis, N. D. McDaniel, S. Bernhard and T. J. Collins, *J. Am. Chem. Soc.***2010**, *132*, 10990-10991; b) J. L. Fillol, Z. Codolà, I. Garcia-Bosch, L. Gómez, J. J. Pla and M. Costas, *Nat. Chem.* **2011**, *3*, 807-813; c) Z. Codolà, I. Gamba, F. Acuña-Parés, C. Casadevall, M. Clémancey, J.-M. Latour, J. M. Luis, J. Lloret-Fillol and M. Costas, *J. Am. Chem. Soc.* **2019**, *141*, 323-333.

[7] a) Z. Codola, L. Gomez, S. T. Kleespies, L. Que, Jr., M. Costas and J. Lloret-Fillol, *Nat. Commun.* **2015**, *6*; b) Z. Codolà, I. Garcia-Bosch, F. Acuña-Parés, I. Prat, J. M. Luis, M. Costas and J. Lloret-Fillol, *Chem. Eur. J.* **2013**, *19*, 8042-8047.

[8] D. G. H. Hetterscheid and J. N. H. Reek, *Eur. J. Inorg. Chem.* **2014**, *2014*, 742-749.

[9] a) A. Company, L. Gómez, X. Fontrodona, X. Ribas and M. Costas, *Chem. Eur. J.* **2008**, *14*, 5727-5731; b) A. Company, L. Gómez, M. Güell, X. Ribas, J. M. Luis, L. Que, Jr and M. Costas, *J. Am. Chem. Soc.* **2007**, *129*, 15766-15767.

[10] O. Planas, M. Clemancey, J.-M. Latour, A. Company and M. Costas, *Chem. Commun.* **2014**, *50*, 10887-10890.

[11] a) Y. Zang, J. Kim, Y. Dong, E. C. Wilkinson, E. H. Appelman and L. Que, Jr., *J. Am. Chem. Soc.* **1997**, *119*, 4197-4205; b) I. Prat, A. Company, T. Corona, T. Parella, X. Ribas and M. Costas, *Inorg. Chem.* **2013**, *52*, 9229−9244-9229−9244.

[12] a) K. Chen and L. Que, *J. Am. Chem. Soc.***2001**, *123*, 6327-6337; b) A. Diebold and K. S. Hagen, *Inorg. Chem.* **1998**, *37*, 215-223; c) G. J. P. Britovsek, J. England and A. J. P. White, *Inorg. Chem.* **2005**, *44*, 8125-8134.

[13] A. Decker, J.-U. Rohde, L. Que, Jr. and E. I. Solomon, *J. Am. Chem. Soc.* **2004**, *126*, 5378-5379.

[14] J.-U. Rohde, J.-H. In, M.-H. Lim, W. W. Brennessel, M. R. Bukowski, A. Stubna, E. Münck, W. Nam and L. Que, Jr., *Science* **2003**, *229*, 1037-1039.

[15] a) A. Y. Kassim and Y. Sulfab, *Inorg. Chem.* **1981**, *20*, 506-509; b) H. A. Ewais, F. D. Dahman and A. A. Abdel-Khalek, *Chem. Cent. J* **2009**, *3*, 3-3; c) H. A. Ewais, M. A. Habib and S. A. K. Elroby, *Trans. Met. Chem.* **2010**, *35*, 73-80.

[16] a) I. Kerezsi, G. Lente and I. Fábián, *Dalton Trans.* **2004**, 342-346; b) L. Valkai, G. Peintler and A. K. Horváth, *Inorg. Chem.* **2017**, *56*, 11417-11425.

[17] a) H. Toftlund, *Coord. Chem. Rev.* **1989**, *94*, 67-108; b) A. Hauser, J. Jeftić, H. Romstedt, R. Hinek and H. Spiering, *Coord. Chem. Rev.* **1999**, *190-192*, 471-491; c) K. P. Kepp, *Inorg. Chem.* **2016**, *55*, 2717-2727; d) D. C. Ashley and E. Jakubikova, *Coord. Chem. Rev.* **2017**, *337*, 97-111; e) H. Petzold, P. Djomgoue, G. Hörner, J. M. Speck, T. Rüffer and D. Schaarschmidt, *Dalton Trans.* **2016**, *45*, 13798-13809; f) B. H. Wilson, H. S. Scott, R. J. Archer, C. Mathonière, R. Clérac and P. E. Kruger, *Magnetochem.* **2019**, *5*, 22.

[18] a) K. P. Bryliakov, E. A. Duban and E. P. Talsi, *Eur. J. Inorg. Chem.* **2005**, *1*, 72-76; b) A. Petuker, K. Merz, C. Merten and U.-P. Apfel, *Inorg. Chem.* **2016**, *55*, 1183-1191; c) B. Strauß, W. Linert, V. Gutmann and R. F. Jameson, *Monatsh. für Chem.* **1992**, *123*, 537-546; d) S. A. Barrett, C. A. Kilner and M. A. Halcrow, *Dalton Trans.* **2011**, *40*, 12021-12024; e) S. A. Barrett and M. A. Halcrow, *Rsc Adv.* **2014**, *4*, 11240-11243; f) K. Keisers, H. M. Hüppe, L. Iffland-Mühlhaus, A. Hoffmann, C. Göbel, U.-P. Apfel, B. Weber and S. Herres-Pawlis, *Inorg. Chem.* **2020**, *59*, 15343-15354.

[19] D. W. Blakesley, S. C. Payne and K. S. Hagen, *Inorg. Chem.* **2000**, *39*, 1979-1989.

[20] M. A. Halcrow, *Dalton Trans.* **2020**.

[21] A. Das, C. Hessin, Y. Ren and M. Desage-El Murr, *Chem. Soc. Rev.* **2020**. doi.org/10.1039/D0CS00914H

[22] R. A. Binstead, et al. in *SPECFIT-32, Spectrum Software Associates: Chappel Hill, 2000.*, *Vol.* **2000**.

Entry for the Table of Contents

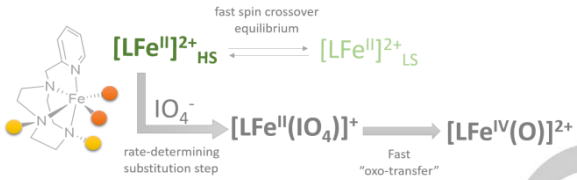

The formation of oxo-iron(IV) complexes from reaction of iron(II) precursors with IO_4^- occurs through a fast spin crossover pre-equilibrium followed by rate-determining substitution to form an intermediate that leads rapidly to the Fe^{IV}=O species. The experimental kinetic and activation parameters highlight a key role of the spin in modulating the reaction.